Quantitative elemental bio-imaging of Mn, Fe, Cu and Zn in 6-hydroxydopamine induced Parkinsonism mouse models

*Dominic Hare[1], Brian Reedy[1], Philip Doble[1]**
Rudolph Grimm[2]
Simon Wilkins[3], Irene Volitakis[3], Jessica L George[3], Robert A Cherny[3], Ashley I Bush[3], David I Finkelstein[3]
[1] Elemental Bio-imaging Facility, University of Technology Sydney, Australia
[2] Agilent Technologies, Santa Clara, USA
[3] Mental Health Research Institute of Victoria, Australia

*** Corresponding Author**

ABSTRACT

This study demonstrates the application of quantitative elemental bio-imaging for the determination of the distribution Cu, Mn, Fe and Zn in Parkinsonism mouse model brains. Elevated concentrations of these metals within the substantia nigra (SN) are suspected to play a role on the development of Parkinson's disease. Elemental bio-imaging employs laser ablation inductively coupled mass spectrometry (LA-ICP-MS) to construct images of trace element distribution. Quantitative data was produced by ablating the standard tissue sections and recording the mean signal intensity calibrated against multi level matrix matched tissue standards. The concentrations of Fe within the substantia nigra of the lesioned animals increased significantly when compared against control animals. Furthermore, the data was compared against solution nebulisation ICP-MS in which the whole substantia nigra was excised. The trends were the same for both methods; however the elemental bio-imaging method returned significantly higher concentrations. This was caused by dilution from inclusion of surrounding tissue of the SN during the excision procedure.

INTRODUCTION

Parkinson's disease (PD) is a degenerative neurological disorder caused by the loss of dopaminergic cells within the pars compacta region of the substantia nigra (SN)[1]. Co-incident with the appearance of symptoms of the disease an elevation of iron has been observed within the SN [2-4]. Iron is suspected to be involved in the formation of reactive oxygen species within the SN, which is hypothesised to lead to the death of dopamine producing cells. It is unclear if the increased oxidative stress caused by Fe in PD is a cause or effect of the disorder[5].

A common mouse model for study of Parkinsonism is the 6-hydroxydopamine (6-OHDA) lesion method. The lesion is produced by directly injecting the neurotoxin into the region of the SN, where it

is taken up by the neurons and kills the cells by the production of active superoxide radicals[6]. Fe is suspected to play a significant role in the mechanism of cell death and superoxide radical generation[2, 3, 7-9].

Development of methods to measure the regional concentration of trace metals in induced Parkinsonism models would be of benefit to probe the mechanism and treatment of PD. Solution nebulisation ICP-MS was employed by Tarohda et al[10]. The SN was excised from 6-OHDA lesioned mouse models and analysed for Mn, Fe, Cu and Zn after closed-vessel microwave digestion. The concentration of Mn, Fe, Cu and Zn increased in the SN to a constant maximum at 7-10 days after injection of the neurotoxin. Solution ICP-MS has also been applied to monitoring iron levels in 1-methyl-4-phenyl-1,2,3,6-tetrahydropyridine (MPTP) treated mice, another mouse model for Parkinsonism[11].

Laser ablation-inductively couple plasma-mass spectrometry (LA-ICP-MS) may be utilised for *in situ* analysis of trace metals in biological tissue. Using a process we term *elemental bio-imaging*, isotope-specific maps of the spatial distribution of trace elements within thin tissue sections can be constructed. ICP-MS is an element analyser, designed to measure trace levels of the elements unlike other forms of "organic" MS that are used to identify and quantify molecular compounds. Laser ablation is a sample introduction system for ICP-MS that allow for the elemental composition of solid materials, including tissues, to be determined.

The biggest limitation of LA-ICP-MS is a lack of reliable validated quantification strategies. Most studies have relied upon certified reference materials or preparation of matrix matched standards. Examples of the former include pig liver paste (LGC 7112) for single point calibration for quantification of trace elements in sheep liver[12]. Jackson *et al*. used pressed pellets of TORT-2 (lobster hepatopancreas), DOLT-2 (dogfish liver) and DORM-2 (dogfish muscle) to build multi-point curves for quantification of Cu, Zn and Fe in rodent brains[13]. Matrix-matched standards have also been prepared by spiking brain tissue with known amounts of aqueous standards and ablating cut sections.[14].

Elemental bio-imaging has also been applied to imaging of P, S and several transition metals in small sized tumours produced by F98 glioma cell implantation in rat brains[15, 16]. Imaging of trace elements in both healthy and tumourous human brain tissue has also been reported[14, 17-19].

This study presents a method to quantify the spatial and regional distribution of Mn, Fe, Cu and Zn in thin tissue sections taken from a 6-OHDA Parkinsonism mouse model, as well as untreated controls. The regional quantification of the substantia nigra obtained by the imaging method was also compared against that obtained by solution nebulisation ICP-MS.

EXPERIMENTAL SECTION

LA-ICP-MS Instrumentation

Experiments were carried out using a New Wave UP213 laser ablation unit (Kenelec Technologies, Mitcham, Victoria, Australia) hyphenated to an Agilent 7500 ce ICP-MS (Agilent Technologies, Forrest Hill, Victoria, Australia) fitted with a 'cs' lens system for enhanced sensitivity. The laser unit was equipped with a frequency quintupled 213 nm Nd:YAG energy source. Typical operational parameters are summarised in Table 1. Argon was used as the carrier gas rather than helium due to its faster washout time. Tissue fissures and inconsistent ablation was minimised by employing low laser power (~0.3 J cm^{-2}). The LA-ICP-MS system was tuned for maximum sensitivity prior to each experiment using NIST 612 Trace Elements in Glass. The ICP-MS was also tuned to minimise the formation of oxides by monitoring the m/z 248/232 ($^{232}Th^{16}O^{+}$ / $^{232}Th^{+}$) ratio. A value of less than 0.2 % for this ratio indicated the signal from potential matrix-based polyatomic interferences was negligible. Furthermore, natural isotopic abundance ratios were monitored to confirm the absence of interfering polyatomic species. Total analysis time per sample was approximately 20 hours. Up to 1 x 10^5 points per measured mass were recorded. Laser scan speed was equal to the laser spot diameter. Thus, the image resolution was equal to the laser spot diameter.

Table 1: Typical parameters for LA-ICP-MS

Agilent 7500ce ICP-MS		**New Wave UP213 Laser Ablation**	
Rf Power	1250W	Wavelength	213 nm
Cooling gas flow rate	15 L min^{-1}	Repetition frequency	20 Hz
Carrier gas flow rate	1.1 L min^{-1}	Laser energy density	0.3 J cm^{-2}
Sample depth	4.0 mm	Spot size	12-30 µm
QP Bias	-5 V	Scan rate	12-30 µm s^{-1}
OctP Bias	-8 V	Line spacing	12-30 µm
Scan mode	Peak hopping	Carrier gas	Ar
Dwell time	0.1 s per m/z		
Measured m/z	13, 31, 55, 56, 57, 63, 66		
Extracts 1, 2	6.8, -126 V		
Reference element (for solution)	$^{103}Rh^{+}$		

Preparation of matrix matched tissue standards

Matrix matched tissue standards were prepared to construct multi-point calibration curves according to the workflow shown in Figure 1. Chicken breast tissue was obtained from a local market and was stripped of all fatty and connective tissue. Approximately 5 g portions of the tissue were spiked with appropriate volumes of 1000 mg L^{-1} Mn, Fe, Cu and Zn standards in 5% HNO_3 (Choice Analytical, Thornleigh, NSW, Australia). A further volume of 5% Seastar Baseline grade HNO_3 (Choice Analytical) was added to a final mass of 6 g to aid homogenisation. Concentration ranges were based on values in both developing rodent brains and 6-OHDA lesioned animals reported by Tarhoda *et al*[10,

[20]. Homogenisation was performed using an OmniTech TH tissue homogeniser fitted with polycarbonate probes (Kelly Scientific, North Sydney, NSW, Australia). 6 aliquots (ca. 100 mg) of accurately weighed homogenised tissue were then digested in 4 : 1 70% Baseline HNO_3 (Choice Analytical) and Ultrapure 31% H_2O_2 (Merck, Kilsyth, Victoria, Australia) using a Milestone MLS 1200 closed vessel microwave digester. The digests were diluted to ca. 50 g with 18.2 mΩ deionised H_2O and its weight accurately recorded.

These solutions were analysed by solution nebulisation ICP-MS using the Agilent 7500 ICP-MS. In brief, mixed standards containing each element were prepared from fresh stocks (Choice Analytical) for calibration. A 250 ppb solution of ^{103}Rh was used as the reference element that was added to each sample via a peristaltic pump and T-piece connector. A quartz concentric nebuliser and Scott-type spray chamber (Glass Expansion, Australia) were used. He was used as a collision gas to remove interferences.

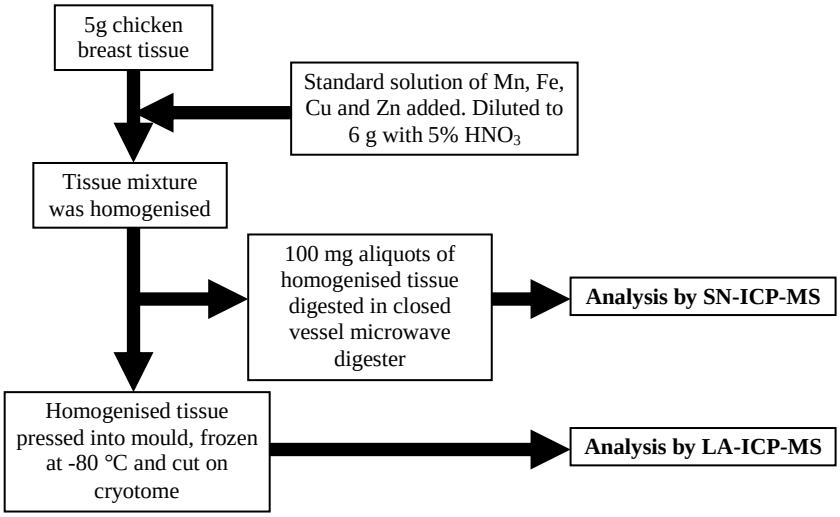

Figure 1: Schematic workflow for standard tissue synthesis.

The homogenised tissue standards were then packed into a 0.5 cm^2 plastic histology moulds and frozen in isopentane/liquid nitrogen. 30 µm thick sections were cut on a cryostat using metal-free PTFE coated C. L. Sturkey Diamond microtome blades (ProSciTech, Kirwan, Qld, Australia).

Animal model

All methods conformed to the Australian National Health and Medical Research Council published code of practice for animal research and was approved by the University of Melbourne Animal Ethics Committee. C57Bl/6 mice were purchased from the Animal Resources Centre (Western Australia). A partial lesion of the SN was produced in the mice by injecting the neurotoxin 6-OHDA into the right SN. The mouse was injected with atropine (0.5 mg/kg, Pharmacia, Australia and xylazine (10 mg/kg, Xylazil-20 Troy Labs., Australia) as premedication. The mouse was initially inducted to anaesthesia with 3-4 % isofluorane (Forthane, Abbott, Australia) carried by oxygen and then maintained at 1.5-2.5

% isofluorane. The head was then secured in a stereotaxic frame with the bite bar 3 mm above horizontal. A solution of 6-OHDA (1.65 mg/ml, Sigma) in ascorbic acid (0.2 mg/ml) was prepared and kept on ice until the time of injection. A 26 gauge needle attached via tubing to a 500 µl syringe (SGE, Australia) mounted in a syringe pump (Bioanalytical Systems Inc., , USA) was inserted into the right SN through a small hole drilled through the top of the skull. The needle was left to settle for 2 min before 2 µl (2.5-3.3 mg, 1.5-1.65 mg/ml) of 6-OHDA was injected slowly (0.5 µl/min) into the right SN (anteroposterior, 3.0 mm; lateral, 1.1 mm; dorsoventral, 4.7 mm, with respect to bregma)[21, 22]. On completion of the injection, the needle was left in place for 2 min then slowly withdrawn at a rate of 1 mm/min. After surgery, the skin was sutured, antiseptic (1 % w/w iodine, Betadine; Faulding and Company, South Australia) was applied to the wound, and the mice were left in a warmed cage to recover. Paracetamol (100 mg/kg) was administered in drinking water as an analgesic after surgery.

Twenty-one days after surgery the animals were killed by an overdose of sodium pentobarbitone (Lethobarb; 100 mg/kg) and perfused with 30 ml of warmed (37 °C) 0.1 M PBS, pH 7.4, followed by 30 ml of chilled 4 % w/v paraformaldehyde (Sigma, St. Louis, MO) and 0.1 M phosphate buffer (4 °C), pH 7.4. The brains were then removed and left at 4 °C overnight in 30 % w/v sucrose in PBS before being frozen and sectioned at 30 µm on a cryostat. Sections were thawed onto glass microscope slides, dried at room temperature and then stored frozen in a desiccator until used. The size of the lesion of the nigra was confirmed by stereological methods in Nissl stained serial sections[22, 23].

Image construction

Single lines of ablation were exported from ChemStation as comma separated value (.csv) format. A macro written in Microsoft Visual Basic was used to normalise each data point to ^{13}C (as recommended by Feldmann *et al* [24]) and combine all data into single ASCII format files. These files were then imported into ITT Visual ENVI 4.2 (Research Systems Inc., Boulder, CO, USA) hyperspectral imaging software package where final images were produced.

Quantitative data was produced by ablating the standard tissue sections and recording the mean signal intensity for each concentration calibrated against the matrix matched tissue standard. Background correction was carried out by subtracting the average signal recorded during a gas blank. ^{13}C standardisation resulted in a higher constant blank slide background for m/z 56 due to $^{40}Ar^{16}O$ formed from O_2 in the plasma gas. Therefore, areas of the image with no tissue present were set to zero.

Solution Nebulisation ICP-MS

Measurements of SN iron levels were assessed by solution ICP-MS according to the method described previously[25]. Briefly, the SN region was dissected, weighed, frozen, lyophilized and then digested overnight in concentrated HNO_3 (Aristar, BDH) before heating at 90°C for 20 min on a heating block. This was followed by the addition of an equivalent amount of 30% (w/v) H_2O_2 Aristar, BDH) to help

dissolve the lipids. The cooled samples were further heated for 15 min at 70 °C. The samples were diluted 1/26 in triplicate with a 1% (v/v) HNO_3 diluent. As controls, preparatory blank tubes (no tissue added) and NIST Standard Reference Material (Bovine liver 1577b, NIST, Gaithersburg, MD) (~10 mg dry wt) were treated in the same manner as the samples.

The metal measurements were made using an UltraMass 700 (Varian Inc., Australia) instrument under normal operating conditions suitable for routine multi-element analysis. Typical operational parameters are summarised in Table 2. The instrument was calibrated using a blank, 10, 50 and 100 ug/L in 1% (v/v) HNO3 of a certified multi-element ICPMS standard solution (AccuStandard Inc., New Haven, CT) containing each element of interest. A certified reference element solution (ICP-MS-IS-MIX1-1, AccuStandard Inc., New Haven, CT) containing 100 ppb of Yttrium (^{89}Y) was added via a T-piece as an internal matrix and instrument performance control. Standards and samples were introduced with a concentric glass nebulizer (K style) (Glass Expansion, Australia) via a peristaltic pump to a Sturman-Masters spray chamber system.

Table 2: Typical parameters for solution ICP-MS.

Varian Ultramass 700 ICPMS			
Rf Power	1200W	Plasma Gas	Ar
Plasma flow	15 L min^{-1}	Aerosol Generation	Nebuliser
Auxiliary flow	1.5 L min^{-1}	Pump rate	10 rpm
Nebulizer flow	0.91 mm	Stabilization time	12 sec
Sample depth	5.0 mm	Extraction Lens	-600 V
Analysis type	Quantitative	Lens: 1, 2, 3, 4	-250, -7.6, 0.8, -80 V
Acquisition Mode	Steady State	Photon Stop	-9 V
Scan mode	Peak hopping	Entrance & Exit Plate	0V
Points/Peak	1	Sample Cones	Nickel
Scans/Replicate	50	Skimmer Cones	Nickel
Replicates/Sample	3	Measured m/z	55, 57, 65, 66
Dwell time	0.01 sec		

RESULTS AND DISCUSSION

Calibration

The matrix matched calibration standards were analysed by solution nebulisation ICP-MS. Both the spiked concentrations and determined concentrations are summarised in Table 3. The amount spiked prior to homogenisation did not necessarily correlate well with the determined concentration. These data demonstrated the requirement for characterisation of the calibration standards prior to quantification of tissue sections.

Table 3: Approximate and determined concentrations of homogenised tissue standards

Standard		Approximate spiked amount (mg kg^{-1})	Measured amount by SN-ICP-MS (mg kg^{-1}) % ± SD (n=6)
1	Mn	1	0.96 ± 0.04
	Fe	10	13.5 ± 2.3
	Cu	1	1.3 ± 0.2
	Zn	10	7.3 ± 1.5
2	Mn	5	4.0 ± 0.2
	Fe	20	17.1 ± 0.9
	Cu	10	7.9 ± 1.0
	Zn	20	26.1 ± 4.2
3	Mn	10	8.5 ± 0.4
	Fe	50	34.2 ± 2.7
	Cu	20	19.7 ± 1.8
	Zn	40	42.5 ± 1.5
4	Mn	20	14.5 ± 0.7
	Fe	100	107.6 ± 8.2
	Cu	50	47.9 ± 3.7
	Zn	60	51.9 ± 5.5

The standard tissue sections were ablated immediately before each sample. Calibration curves for each isotope were constructed by plotting the signal intensity after ^{13}C normalization against the determined concentration. Table 4 details typical calibration data after laser ablation. All calibration curves showed good linearity within the chosen concentration range. The y intercepts for all the measured elements (except Fe) passed approximately through the origin which indicated low background counts. The high y - intercept of Fe was due to the *background* polyatomic interference of $^{40}Ar^{16}O^{+}$.

Table 4: Calibration Data

Isotope	Correlation Coefficient (r^2)	Slope (± 95% CI) x 10^{-4}	Intercept (± 95% CI) x 10^{-3}
^{55}Mn	0.9878	245 ± 50	19 ± 38
^{56}Fe	0.9997	128.3 ± 4.1	1193 ± 21
^{63}Cu	0.9993	48.7 ± 2.5	15.0 ± 5.8
^{66}Zn	0.9736	9.1 ± 2.8	4.2 ± 9.0

Using the above linear regression, each data point (or pixel) in ENVI was converted from an intensity/^{13}C ratio to mg kg^{-1} concentration, allowing the production of quantitative images at 30 μm resolution. Areas of interest were also quantified by built in functions in ENVI software.

6-OHDA lesioned animals

The lesion procedure resulted in a loss of between 50% and 66% of SN neurons. Figure 2 shows the quantitative ^{56}Fe image of a 6-OHDA lesioned brain at 30 μm resolution. The ^{56}Fe concentrations generally ranged from 39 to 67 mg kg^{-1}, although the area in the region of the needle track corresponded to concentrations as high as 120 mg kg^{-1}. The most likely explanation for the elevated ^{56}Fe concentrations was heme residue from blood released by placing the needle into the brain. This image shows the strength of this method of analysis, in that, the area surrounding the needle tract can be excluded from analysis. All previous methods to date (chemical and tissue samples analysed by solution - ICP-MS) would have included the artifact of the method in the data.
There was also considerable increase in Fe concentration within the region of the SN on the lesioned hemisphere when compared to the unlesioned hemisphere. The $^{56}Fe/^{57}Fe$ ratio did not significantly deviate from the natural isotopic abundance pattern, indicating *matrix* interference due to the production of $^{40}Ar^{16}O^{+}$ was negligible.

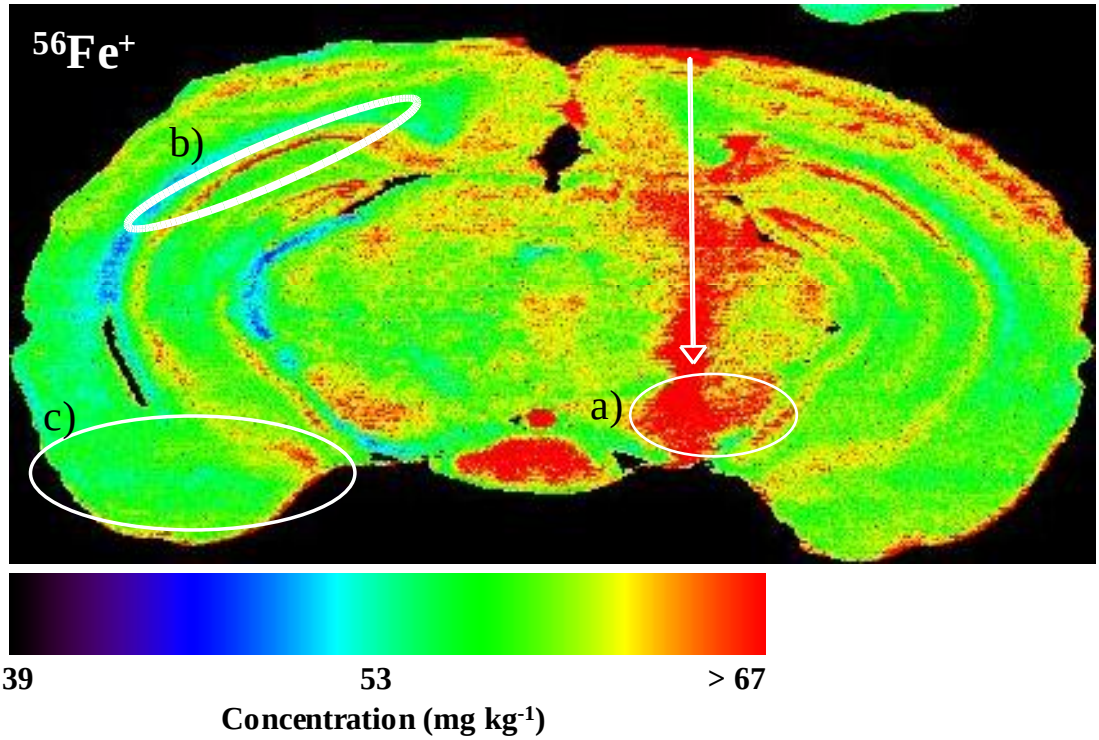

Figure 2: ^{56}Fe image of 6-OHDA lesioned mouse brain at the level of the SN. The needle track is shown by the white arrow. a) = substantia nigra, b) = dentate gyrus, c) = amygdala and hippocampus.

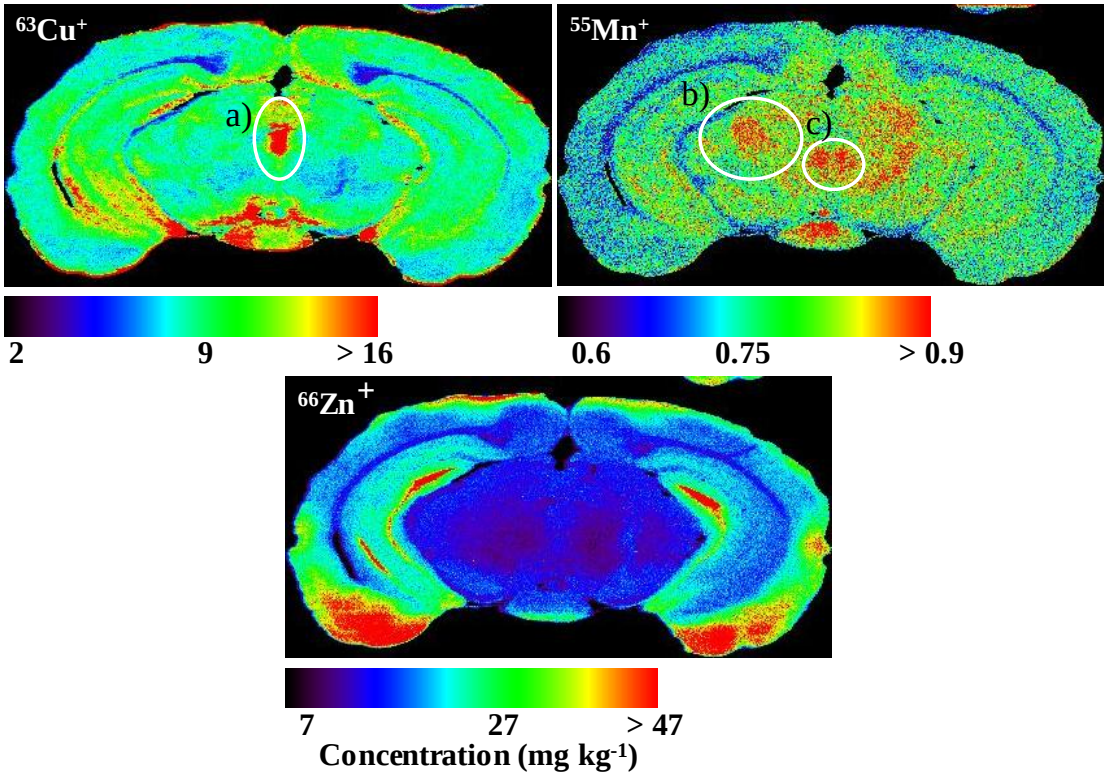

Figure 3: ^{63}Cu, ^{55}Mn and $^{66}Zn^{+}$ images of 6-OHDA lesioned animal. a) = superior colliculus, b) = anterior pretectal and medial geniculate nucleus, c) = medial accessory oculomotor nucleus.

Figure 3 shows ^{63}Cu, ^{55}Mn and ^{66}Zn images. The ^{63}Cu bilateral concentrations were up to 80 mg kg^{-1} about the 3rd ventricle and 25-35 mg kg^{-1} in the region of the commissure of the superior colliculus. The bilateral concentration of Zn was approximately 25 mg kg^{-1} in the hippocampus. ^{55}Mn was consistently distributed through the brain section, with slightly higher concentrations within anterior pretectal, medial accessory oculomotor and medial geniculate nuclei nucleus. Bilaterally higher concentrations of ^{66}Zn were seen within the amygdala and hippocampal regions (up to 60 mg kg^{-1}), as well as along the dentate gyrus (DG). The concentration of ^{66}Zn also increased at the base of the needle track. Concentrations of ^{66}Zn above 50 mg kg^{-1} were extrapolated from the linear regression analysis due to concentration values falling outside the standard range.

Higher resolution images were constructed from a separate lesioned animal surrounding the region of the SN and are shown in Figure 4. Ablation was performed with a beam diameter of 12 µm and scan speed of 12 µm s^{-1}. The laser power was increased to approximately 0.5 J cm^{-2} without the formation of fissures in the tissue, or large particles. The signal from Fe associated with the needle track was set to zero for image clarity. The SN is clearly seen, however the contrast is not as dramatic as in Figure 3 due to the narrower concentration range displayed. A three dimensional view of the 12 um resolution scan is shown in Figure 5. The SN is clearly seen and some fine detail in Fe distribution can be discerned.

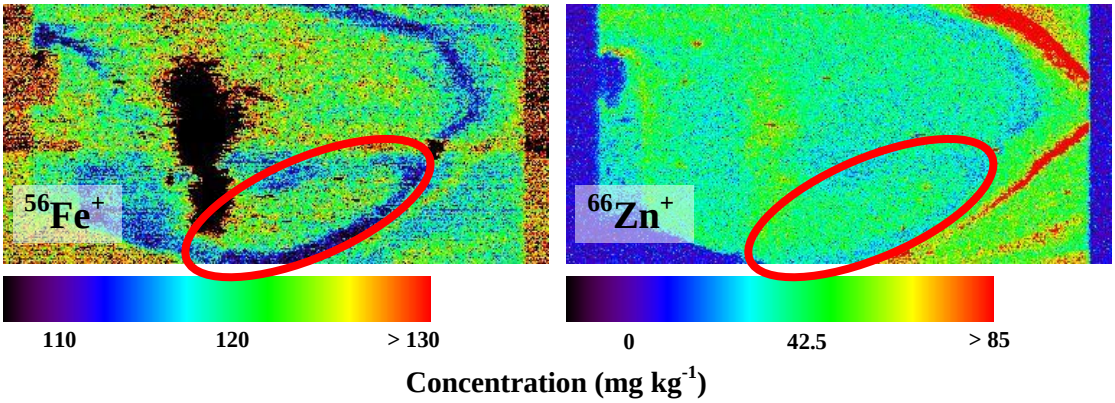

Figure 4: 12 µm resolution ^{56}Fe and ^{66}Zn images of 6-OHDA lesioned animal. The signal due to high Fe concentrations surrounding the needle track was set to zero for image clarity.

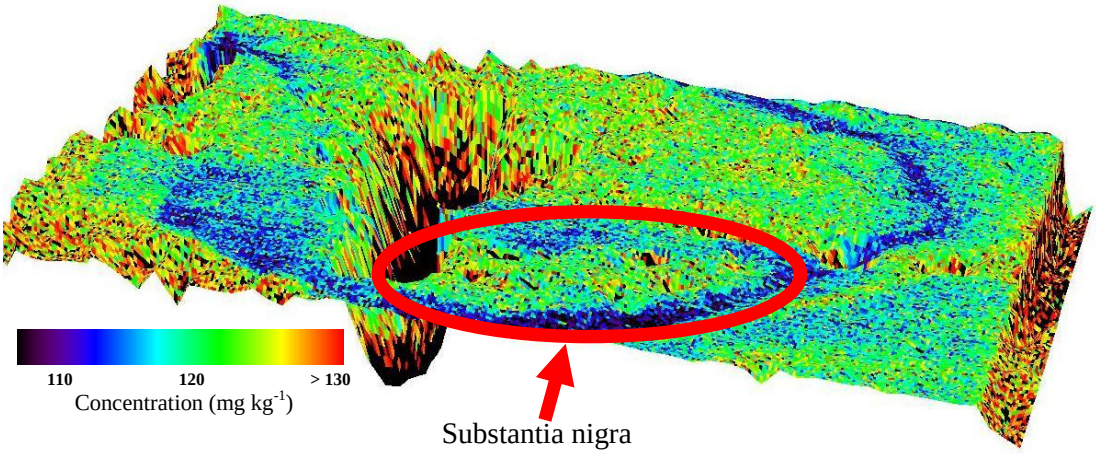

Figure 5: Three-dimensional surface view of ^{56}Fe 12 µm resolution image.

Tarohda *et al* [10] reported a range in Fe concentration within the SN from 20 to greater than 200 mg kg^{-1}. The concentrations determined in this animal model were in agreement with these values indicating that the quantification method shows good potential for detailed studies of iron distributions in PD models.

Control animals

Comparisons of the 6-OHDA animals were made against control animals. Mean Fe concentrations within the substantia nigra are presented in Table 5. Lesioned animals displayed a bilateral increase in mean Fe concentration compared to the control. A bilateral decease in the number of SN neurons has been reported previously from a unilateral injection of toxin[26]. This is thought to be caused by spread of the toxin within the brain. Regional distributions of ^{63}Cu, ^{55}Mn and ^{66}Zn were comparable to those seen in the lesioned animals. The Fe concentrations determined from the digested samples analysed by solution nebulisation ICP-MS show the same trends but significantly lower concentrations. This was caused by dilution from the surrounding tissue of the SN by the excision procedure.

Table 5: Comparison of Fe concentrations within the SN by LA-ICP-MS and SN-ICP-MS.

	Right Hemisphere (mg kg^{-1})		**Left Hemisphere (mg kg^{-1})**	
	LA-ICP-MS	**SN-ICP-MS**	**LA-ICP-MS**	**SN-ICP-MS**
6-OHDA lesion* (right hemisphere) 3 animals, 1 section)	90.1 ± 11.9 (n=3)	17.1 ± 1.7 (n=5)	84.3 ± 10.3 (n=3)	18.9 ± 4.0 (n=5)
Control (1 animal, 2 sections)	37.7 ± 7.1 (n=2)	13.2 ± 3.2 * (n=6)	25.6 ± 7.9 (n=2)	13.2 ± 3.2 * (n=6)
*Bilateral determination				

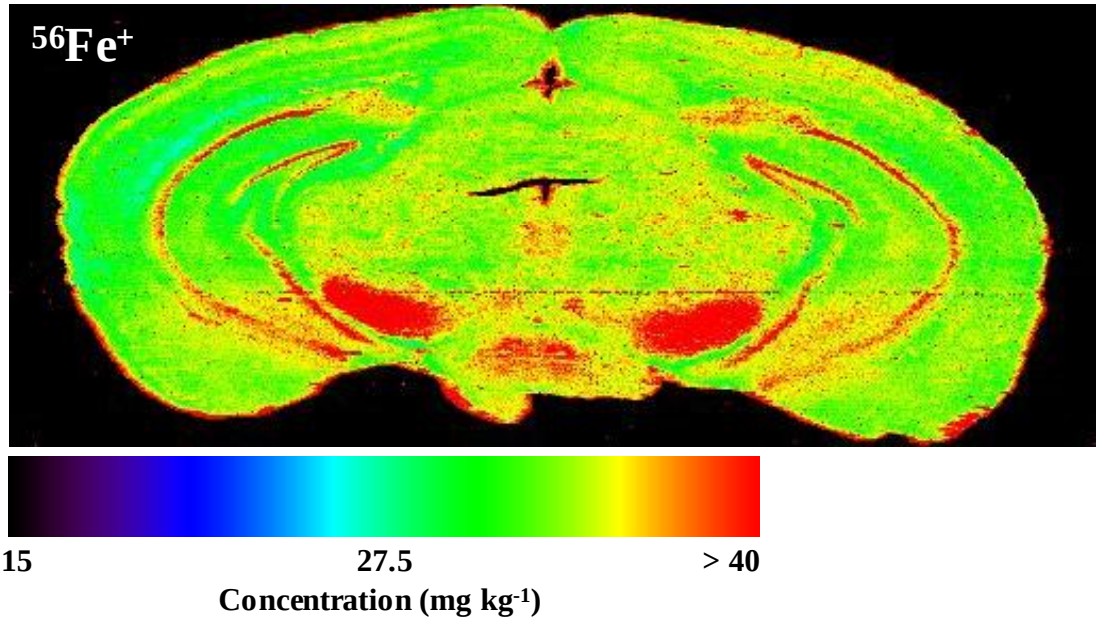

Figure 6: ^{56}Fe image of control animal

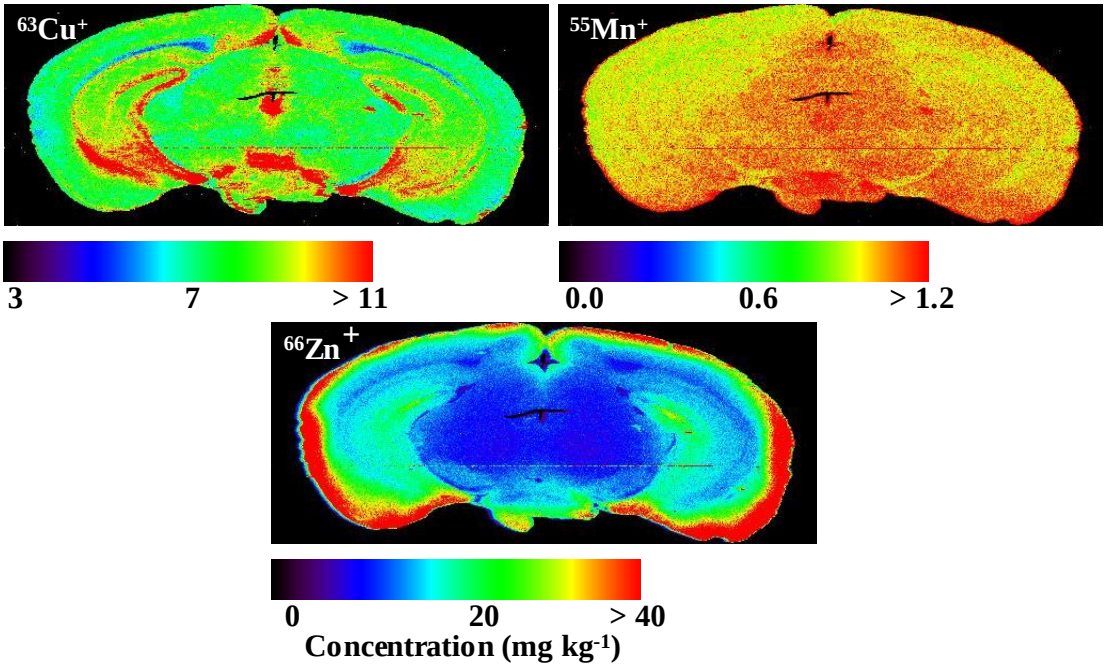

Figure 7: ^{63}Cu, ^{55}Mn and ^{66}Zn images of control animal.

Immunohistochemical staining for tyrosine hydroxylase (TH) activity was performed and is shown in Figure 8. TH is an enzyme that converts tyrosine to dihydroxyphenylalanaine (L-DOPA) and is an essential part of the dopamine pathway. TH activity is indicative of the presence of normal functioning dopamine producing cells within the SN. This region correlated well with the increased concentrations of ^{56}Fe shown in Figures 6 and 7. This demonstrates that the correct sections were selected for elemental bio-imaging and that changes in metal related to the SN.

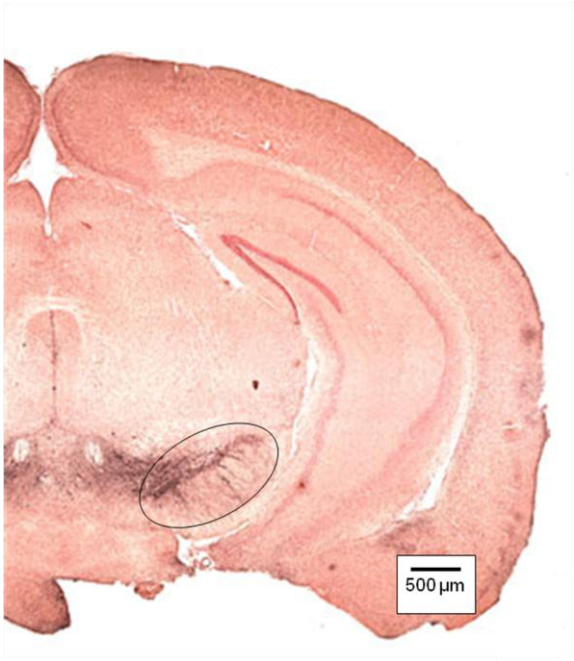

Figure 8: Immunohistochemical stain showing tyrosine hydroxylase activity in a control animal. The circle shows area of TH activity (black) corresponding with the area of the SN. This section is the next serial section to that shown in Figures 6& 7.

CONCLUSION

We have demonstrated that matrix-matched tissue standards were suitable for quantifying trace metals in thin tissue sections. The method was applied to quantify the regional concentration of Fe, Cu, Zn and Mn in a 6-OHDA lesion mouse model for Parkinsonism. The results showed that unilateral 6-OHDA lesioning increased the concentration of ^{56}Fe bilaterally within the substantia nigra when compared against control animals. The quantification data obtained from the LA-ICP-MS was compared against that obtained from excision and solution nebulisation ICP-MS. The trends were the same for both methods; however the concentrations for Fe were significantly higher when determined by the LA-ICP-MS method. This method allowed direct sampling of small regions of the mouse brain without the need for dissection and digestion of the region of interest. The elevation of iron within the substantia nigra has become significant for researchers investigating the Parkinson's disease. Elemental bio-imaging is a novel and potential valuable tool in the quest for understanding the biological processes occurring in PD.

ACKNOWLEDGEMENT

The authors gratefully acknowledge the assistance of the NSW Department of Forensic Medicine (Sydney, NSW, Australia) for their valuable advice and experience.

1. M. S. Ebadi and R. Pfeiffer, *Parkinson's Disease*, CRC Press, Boca Raton, 2005.
2. D. Berg, *Neurochem Res*, 2007, **32**, 1646-1654.

3. A. Gaenslen, B. Unmuth, J. Godau, I. Liepelt, A. Di Santo, J. Schweitzer Katherine, T. Gasser, H.-J. Machulla, M. Reimold, K. Marek and D. Berg, *Lancet Neurol*, 2008, **7**, 417-424.
4. D. Kaur and J. K. Andersen, *Aging Cell*, 2002, **1**, 17-21.
5. P. M. Doraiswamy and A. E. Finefrock, *Lancet Neurol*, 2004, **3**, 431-434.
6. A. Schober, *Cell Tissue Res*, 2004, **318**, 215-224.
7. Y. He, P. S. P. Thong, T. Lee, S. K. Leong, C. Y. Shi, P. T. H. Wong, S. Y. Yuan and F. Watt, *Brain Res*, 1996, **735**, 149-153.
8. E. Oestreicher, G. J. Sengstock, P. Riederer, C. W. Olanow, A. J. Dunn and G. W. Arendash, *Brain Res*, 1994, **660**, 8-18.
9. S. Michaeli, G. Oz, J. Sorce Dennis, M. Garwood, K. Ugurbil, S. Majestic and P. Tuite, *Movement Disord*, 2007, **22**, 334-340.
10. T. Tarohda, Y. Ishida, K. Kawai, M. Yamamoto and R. Amano, *Anal Bioanal Chem*, 2005, **383**, 224-234.
11. D. Kaur, F. Yantiri, S. Rajagopalan, J. Kumar, J. Q. Mo, R. Boonplueang, V. Viswanath, R. Jacobs, L. Yang, M. F. Beal, D. DiMonte, I. Volitaskis, L. Ellerby, R. A. Cherny, A. I. Bush and J. K. Andersen, *Neuron*, 2003, **37**, 899-909.
12. A. Kindness, N. Sekaran Chandra and J. Feldmann, *Clin Chem*, 2003, **49**, 1916-1923.
13. B. Jackson, S. Harper, L. Smith and J. Flinn, *Anal and Bioanal Chem*, 2006, **384**, 951-957.
14. J. S. Becker, M. V. Zoriy, C. Pickhardt, N. Palomero-Gallagher and K. Zilles, *Anal Chem*, 2005, **77**, 3208-3216.
15. M. V. Zoriy, M. Dehnhardt, A. Matusch and J. S. Becker, *Spectrochim Acta B*, 2008, **63**, 375-382.
16. J. S. Becker, M. V. Zoriy, M. Dehnhardt, C. Pickhardt and K. Zilles, *J Anal Atom Spectrom*, 2005, **20**, 912-917.
17. J. Dobrowolska, M. Dehnhardt, A. Matusch, M. Zoriy, N. Palomero-Gallagher, P. Koscielniak, K. Zilles and J. S. Becker, *Talanta*, 2008, **74**, 717-723.
18. M. V. Zoriy and J. S. Becker, *Int J Mass Spectrom*, 2007, **264**, 175-180.
19. M. V. Zoriy, M. Dehnhardt, G. Reifenberger, K. Zilles and J. S. Becker, *Int J Mass Spectrom*, 2006, **257**, 27-33.
20. T. Tarohda, M. Yamamoto and R. Amamo, *Anal Bioanal Chem*, 2004, **380**, 240-246.
21. K. B. J. Franklin and G. Paxinos, *The mouse brain in stereotaxic coordinates*, Academic Press, San Diego, 1997.
22. C. L. Parish, D. I. Finkelstein, J. Drago, E. Borrelli and M. K. Horne, *J Neurosci*, 2001, **21**, 5147-5157.
23. D. Finkelstein, I., D. Stanic, C. Parish, L., J. Drago and M. Horne, K., *Curr Prot Neurosci*, 2004, **Chapter 1**, Unit 1 13.
24. J. Feldmann, A. Kindness and P. Ek, *J Anal Atom Spectrom*, 2002, **17**, 813-818.
25. C. J. Maynard, R. Cappai, I. Volitakis, R. A. Cherny, C. L. Masters, Q.-X. Li and A. I. Bush, *J. Inorg. Biochem.*, 2006, **100**, 952-962.
26. D. I. Finkelstein, D. Stanic, C. L. Parish, D. Tomas, K. Dickson and M. K. Horne, *Neuroscience*, 2000, **97**, 99-112.